*Journal of the Korean Nuclear Society*
*Volume 28, Number 3, pp. 311~319, June 1996*

# On the Reconstruction of Pinwise Flux Distribution Using Several Types of Boundary Conditions

**C.J. Park, Y.H. Kim, and N.Z. Cho**
Korea Advanced Institute of Science and Technology
Department of Nuclear Engineering
373-1 Kusong-dong, Yusong-gu, Taejon 305-701, Korea

(Received December 26, 1995)

## Abstract

We reconstruct the assembly pinwise flux using several types of boundary conditions and confirm that the reconstructed fluxes are the same with the reference flux if the boundary condition is exact. We test EPRI-9R benchmark problem with four boundary conditions, such as Dirichlet boundary condition, Neumann boundary condition, homogeneous mixed boundary condition (albedo type), and inhomogeneous mixed boundary condition. We also test reconstruction of the pinwise flux from nodal values, specifically from the AFEN [1, 2] results. From the nodal flux distribution we obtain surface flux and surface current distributions, which can be used to construct various types of boundary conditions. The results show that the Neumann boundary condition cannot be used for iterative schemes because of its ill-conditioning problem and that the other three boundary conditions give similar accuracy. The Dirichlet boundary condition requires the shortest computing time. The inhomogeneous mixed boundary condition requires only slightly longer computing time than the Dirichlet boundary condition, so that it could also be an alternative. In contrast to the fixed-source type problem resulting from the Dirichlet, Neumann, inhomogeneous mixed boundary conditions, the homogeneous mixed boundary condition constitutes an eigenvalue problem and requires longest computing time among the three (Dirichlet, inhomogeneous mixed, homogeneous mixed) boundary condition problems.

### 1. Introduction

To obtain homogenized cross sections, many homogenization methods have been developed until recently. Among several methods, Koebke's "Equivalence Theory" [3] and Smith's "Generalized Equivalence Theory" [4] are most popular. These methods introduce the heterogeneity factor and discontinuity factor. Such homogenized cross sections are used in nodal calculation that is very accurate and fast. After nodal calculation, we need to reconstruct pinwise flux from the nodal values, such as the volume average flux, surface average fluxes, and corner-point fluxes. One of the reconstruction methods is to find the boundary condition as flux or current distribution from such nodal values and then perform fine-mesh calculation [5, 6].

The error in the boundary condition leads to discrepancy in the reconstructed flux with respect to the original reference flux. So reducing the error in the

boundary condition is very important in reconstruction. If the boundary flux or current is exact, then the reconstructed flux would have no error.

The objective of this paper is two-fold. First, we want to confirm numerically that if the boundary condition is exact then the reconstructed pinwise flux is the same with the original flux, regardless of the types of boundary conditions used. We test four boundary conditions, i.e., (1) Dirichlet boundary condition, (2) Neumann boundary condition, (3) inhomogeneous mixed boundary condition, and (4) homogeneous mixed boundary condition, with the EPRI-9R benchmark problem. We also compare these results in terms of computing time and spectral radius of the Jacobi matrix. Second, we like to assess the efficiency of the various boundary conditions when used in the reconstruction of nodal results.

We reconstruct the pinwise flux with AFEN [1, 2] results of the EPRI-9R benchmark problem and compare pin flux peak error and computing time of the boundary conditions.

In Section 2, we derive the finite difference matrix equations when several types of boundary conditions are used. In Section 3, we derive the nodal surface flux distribution from the AFEN fluxes. In Section 4, we show the EPRI-9R results obtained using the exact boundary condition and the various boundary conditions. Finally, we provide conclusions in Section 5.

## 2. Derivation of Difference Equations with Several Boundary Conditions

We calculate pinwise heterogeneous flux by fine-mesh finite difference method with exact boundary condition. Consider the following two-dimensional two-group diffusion equation :

$$-\nabla \cdot D_g \nabla \phi_g(x,y) + \Sigma_{tg}\phi_g = \sum_{g'=1}^{2} (\Sigma_{gg'} + \frac{\chi_g}{k_{eff}} \nu\Sigma_{fg'})\phi_{g'} \quad (1)$$

After differencing the above equation in mesh box (i, j) with standard box scheme, the difference equation becomes

$$J_g^L + J_g^R + J_g^T + J_g^B + \Sigma_{tg}\,\bar{\phi}_{gi,j}\Delta x_i \Delta y_j = \sum_{g'=1}^{2} (\Sigma_{gg'} + \frac{\chi_g}{k_{eff}} \nu\Sigma_{fg'})\,\bar{\phi}_{g'i,j}\Delta x_i \Delta y_j \quad (2)$$

where $\bar{\phi}_{gi,j}$ denotes the average of $\bar{\phi}_g$ in mesh box (i, j) and other notations are standard as used in reference 7. The surface integrated current terms (left, right, bottom, top) are approximated as

$$\begin{aligned} J_g^L &= a_{gi,j}^L (\bar{\phi}_{gi-1,j} - \bar{\phi}_{gi,j}), \\ J_g^R &= a_{gi,j}^R (\bar{\phi}_{gi+1,j} - \bar{\phi}_{gi,j}), \\ J_g^B &= a_{gi,j}^B (\bar{\phi}_{gi,j-1} - \bar{\phi}_{gi,j}), \\ J_g^T &= a_{gi,j}^T (\bar{\phi}_{gi,j+1} - \bar{\phi}_{gi,j}), \qquad g = 1,2, \end{aligned} \quad (3)$$

where

$$\begin{aligned} a_{gi,j}^L &= \frac{-2\Delta y_j}{\Delta x_{i-1}/D_{gi-1,j} + \Delta x_i/D_{gi,j}}, \\ a_{gi,j}^R &= \frac{-2\Delta y_j}{\Delta x_{i+1}/D_{gi+1,j} + \Delta x_i/D_{gi,j}}, \\ a_{gi,j}^B &= \frac{-2\Delta x_i}{\Delta y_{j-1}/D_{gi,j-1} + \Delta y_j/D_{gi,j}}, \\ a_{gi,j}^T &= \frac{-2\Delta x_i}{\Delta y_{j+1}/D_{gi,j+1} + \Delta y_i/D_{gi,j}}. \end{aligned} \quad (4)$$

Here $\Delta x_i$, $\Delta y_j$, are fine mesh sizes of $x$ and $y$ directions. Rearranging all the terms, Eq.(2) becomes the following matrix equation :

$$A\Phi = \frac{1}{k_{eff}} F\Phi. \quad (5)$$

Now we want to reconstruct the pinwise flux using the form of Eq.(5). As a matter of principle, we want to confirm numerically the theoretically known fact that if the boundary condition is exact then the reconstructed flux is the same with the original flux under the same finite difference scheme, regardless of the types of boundary conditions used. Usually we want to reconstruct pinwise flux from the nodal fluxes and multiplication factor.

When we reconstruct pinwise flux, the form of Eq.

(5) is modified. The terms containing the unknowns are left in the left hand side and the knowns as the boundary conditions are moved to the right hand side of the equation. Afterall the problem changes into a fixed-source problem. So the diagonal components of the matrix are changed, which affect convergence of the iteration system. The diagonal dominance is reduced because the diagonal term of the right term is subtracted from the diagonal term of the left term in Eq.(5). In special cases, the spectral radius of the Jacobi matrix becomes bigger than one and this is a serious situation in that the usual iterative schemes (Jacobi, Gauss-Seidel, and SOR) do not work. We experienced such cases sometimes when we use the Neumann boundary condition, so a direct inversion scheme such as Gauss-Jordan method must be used as a solver.

### 2.1. Dirichlet Boundary Condition

First, we can easily think that the surface flux can be used as a boundary condition. In the case of nodal methods, we also need to consider discontinuity factors on the surfaces of a node.

After the surface flux distribution is found, we modify Eq.(5). If we edit at the left boundary surface, the equation can be expressed as follows :

$$a^{R}_{gi,j}\,\bar{\phi}_{gi+1,j} + a^{B}_{gi,j}\,\bar{\phi}_{gi,j-1} + a^{T}_{gi,j}\,\bar{\phi}_{gi,j+1} + a^{C}_{gi,j}\,\bar{\phi}_{gi,j} \qquad (7)$$

$$-\sum_{g'=1}^{2}\left(\Sigma_{gg'} + \frac{\chi_g}{k_{eff}}\nu\Sigma_{fg'}\right)\bar{\phi}_{g'ij}\Delta x_i\Delta y_j = c_{sg}\phi_{sg,j},$$

where

$$a^{C}_{gi,j} = \Sigma_{tg}\,\bar{\phi}_{gi,j}\Delta x_i\Delta y_j + c_{sg} - a^{R}_{gi,j} - a^{B}_{gi,j} - a^{T}_{gi,j}. \qquad (8)$$

Here $c_{s1}$, $c_{s2}$ are calculated from the definition of current in a usual finite difference scheme as follows :

$$J^{L}_{g} = -D_{gi,j}\frac{(\phi_{sg,j} - \bar{\phi}_{gi,j})}{\Delta x_i/2}\Delta y_j = -c_{sg}(\phi_{sg,j} - \bar{\phi}_{gi,j}), \qquad (9)$$

where

$$c_{sg} = \frac{2D_{gi,j}\,\Delta y_j}{\Delta x_i}. \qquad (10)$$

Then we can transform Eq.(7) into matrix form which is a fixed-source problem such as

$$A^{f}\,\Phi = S^{f}. \qquad (11)$$

As $c_{s1}$, $c_{s2}$ are added to the diagonal term, the matrix $A^{f}$ becomes more diagonally dominant than the Neumann boundary condition case in the next section. We can easily solve Eq.(11) by a standard iterative method.

### 2.2. Neumann Boundary Condition

Many people used current as a boundary condition in reconstruction because current continuity condition is preserved when nodal calculation is performed. This formulation is very prone to ill-conditioning situation. We also find in some cases that the spectral radius of the Jacobi matrix is greater than one and thus the usual iterative methods do no converge. So we solve the equation by Gauss-Jordan method, which is a popular direct inverse scheme. The derivation of the equation is similar to that of the Dirichlet boundary condition. The equation at the left surface boundary is given as follows :

$$a^{R}_{gi,j}\,\bar{\phi}_{gi+1,j} + a^{B}_{gi,j}\,\bar{\phi}_{gi,j-1} + a^{T}_{gi,j}\,\bar{\phi}_{gi,j+1} + a^{C}_{gi,j}\,\bar{\phi}_{gi,j} \qquad (12)$$

$$-\sum_{g'=1}^{2}\left(\Sigma_{gg'} + \frac{\chi_g}{k_{eff}}\nu\Sigma_{fg'}\right)\bar{\phi}_{g'ij}\Delta x_i\Delta y_j = J_{sg,j},$$

where

$$a^{C}_{gi,j} = \Sigma_{tg}\,\bar{\phi}_{gi,j}\Delta x_i\,\Delta y_j - a^{R}_{gi,j} - a^{B}_{gi,j} - a^{T}_{gi,j}. \qquad (13)$$

Here $J_{s1,j}$, $J_{s2,j}$, denote fast and thermal surface integrated currents ($j$ th node), respectively.

We can also represent Eq.(12) as

$$A^{c}\,\Phi = S^{c}. \qquad (14)$$

We can infer that diagonal dominance of $A^c$ can be lost or may not be so strong compared with that of the matrix associated with the Dirichlet boundary condition. This is due to the lack of the $c_{sg}$ term in Eq. (13), in contrast to Eq.(8). So we do not recommend the use of the current boundary condition.

### 2.3. Mixed Boundary Condition

Kim and Cho [8] found that if a mixed boundary condition is used, the diagonal dominance can be maintained. There are two kinds of mixed boundary conditions, that is, inhomogeneous case and homogeneous case.

#### i) Inhomogeneous case

The inhomogeneous mixed boundary condition is given as follows :

$$\alpha J_{sg}+\beta\phi_{sg} = \gamma_g. \tag{15}$$

With chosen $\alpha$ and $\beta$, we can derive the following equation, e.g., at the left boundary surface :

$$a^R_{gi,j}\,\bar{\phi}_{gi+1,j} + a^B_{gi,j}\,\bar{\phi}_{gi,j-1} + a^T_{gi,j}\,\bar{\phi}_{gi,j+1} + a^C_{gi,j}\,\bar{\phi}_{gi,j} \tag{16}$$

$$-\sum_{g'=1}^{2}\left(\Sigma_{gg'}+\frac{\chi_g}{k_{eff}}\nu\Sigma_{fg'}\right)\bar{\phi}_{g'ij}\Delta x_i\Delta y_j = w_{sg},$$

where

$$a^C_{gi,j} = \Sigma_{tg}\,\bar{\phi}_{gi,j}\Delta x_i\Delta y_j - a^R_{gi,j} - a^B_{gi,j} - a^T_{gi,j} + z_{sg}. \tag{17}$$

We can derive constants $z_{sg}$ and $w_{sg}$ as follows.

First, we write current as

$$J^L_g = -D_{gi,j}\frac{(\phi_{sg,j}-\bar{\phi}_{gi,j})}{\Delta x_i/2}\Delta y_j = \frac{\gamma_g-\beta\phi_{sg,j}}{\alpha}. \tag{18}$$

From Eq.(18), we find the following expression for the left surface flux :

$$\phi_{sg,j} = \frac{\alpha D_{gi,j}\Delta y_j\,\bar{\phi}_{i,j}-\gamma_g\Delta x_i/2}{\alpha D_{gi,j}\Delta y_j-\beta\Delta x_i/2}. \tag{19}$$

Then, we have the following equation from Eqs. (18) and (19) :

$$\begin{aligned} J^L_g &= \frac{1}{\alpha}(\gamma_g-\beta\phi_{sg,j}) \\ &= \frac{1}{\alpha}\left(\gamma_g-\beta\frac{\alpha D_{gi,j}\Delta y_j\,\bar{\phi}_{i,j}-\gamma_g\Delta x_i/2}{\alpha D_{gi,j}\Delta y_j-\beta\Delta x_i/2}\right) \\ &= \frac{\gamma_g D_{gi,j}\Delta y_j-\beta D_{gi,j}\Delta y_j\,\bar{\phi}_{i,j}}{\alpha D_{gi,j}\Delta y_j-\beta\Delta x_i/2} \\ &= z_{sg}\,\bar{\phi}_{i,j}+w_{sg} \end{aligned} \tag{20}$$

where $z_{sg}$ and $w_{sg}$ are defined as

$$\begin{aligned} z_{sg} &= \frac{\beta D_{gi,j}\Delta y_j}{(\beta\Delta x_i/2-\alpha D_{gi,j})}, \\ w_{sg} &= \frac{\gamma_g D_{gi,j}\Delta y_j}{(\beta\Delta x_i/2-\alpha D_{gi,j})}. \end{aligned} \tag{21}$$

We have the following matrix equation that is also a fixed-source problem :

$$A^i\,\Phi = S^i. \tag{22}$$

We can adjust $\alpha$ and $\beta$ to provide strong diagonal dominance to $A^i$, so this is a well-posed problem for iterative solution.

#### ii) Homogeneous case

The homogeneous boundary condition is given to the ratio of current to flux (albedo type) :

$$J_{sg}/\phi_{sg} = \gamma_g. \tag{23}$$

In this case, the reconstruction problem becomes an eigenvalue problem. Thus, we consider inner and outer iterations with acceleration schemes.

We can derive the following equation at the left boundary surface :

$$a^R_{gi,j}\,\bar{\phi}_{gi+1,j} + a^B_{gi,j}\,\bar{\phi}_{gi,j-1} + a^T_{gi,j}\,\bar{\phi}_{gi,j+1} + a^C_{gi,j}\,\bar{\phi}_{gi,j}$$

$$= \sum_{g'=1}^{2} (\Sigma_{gg} + \frac{\chi_g}{\lambda} \nu\Sigma_{fg'}) \bar{\phi}_{g'i,j} \Delta x_i \Delta y_j, \quad (24)$$

where

$$a^C_{gi,j} = \Sigma_{tg} \bar{\phi}_{gi,j} \Delta x_i \Delta y_j - a^R_{gi,j} - a^B_{gi,j} - a^T_{gi,j} + u_{sg}. \quad (25)$$

Now we can derive $u_{s1}$ and $u_{s2}$ as follows.

First, we write current as

$$J^L_g = -D_{gi,j} \frac{(\phi_{sg,j} - \bar{\phi}_{gi,j})}{\Delta x_i/2} \Delta y_j = \gamma_g \phi_{sg,j}. \quad (26)$$

Then the flux at the left surface is expressed as

$$\phi_{sg,j} = \frac{D_{gi,j} \Delta y_j}{D_{gi,j} \Delta y_j + \gamma_g \Delta x_j/2} \quad (27)$$

Rewrite $J^L_g$,

$$J^L_g = \gamma_g \phi_{sg,j} = \frac{\gamma_g D_{gi,j} \Delta y_j}{D_{gi,j} \Delta y_j + \gamma_g \Delta x_j/2} \bar{\phi}_{gi,j} = u_{sg} \bar{\phi}_{gi,j}, \quad (28)$$

where

$$u_{sg} = \frac{\gamma_g D_{gi,j} \Delta y_j}{D_{gi,j} \Delta y_j + \gamma_g \Delta x_i/2} \quad (28)$$

Finally, we get the following eigenvalue problem in matrix form :

$$A^h \Phi = \frac{1}{\lambda} F^h \Phi. \quad (29)$$

We have verified that the eigenvalue $\lambda$ has the same value as the reference multiplication factor $k_{eff}$ if we use the ratio of exact surface current to flux as the boundary condition. If the boundary condition has some error, $\lambda$ deviates from the reference multiplication factor. In contrast to the fixed-source problems, we must re-normalize single assembly pin flux using nodal power because of the nature of the eigenvlaue problem. Thus the reconstructed pinwise flux also contains some errors resulting from the error of nodal assembly power. But the error of reconstructed flux tends to be small because the nodal power is usually more accurate than the boundary condition and $\lambda$ adjusts itself to the eigen system.

## 3. Reconstruction with AFEN Results

The Analytic Function Expansion Nodal (AFEN) method [1, 2] does not use the transverse integration and represents the multi-dimensional flux in terms of analytic basis functions. So the AFEN method provides good accuracy in realistic problems.

Here, we use the AFEN representation to find the surface boundary condition from AFEN values ; the node-average flux, the node interface fluxes, and the corner-point fluxes. We also have the multiplication factor $k_{eff}$.

With these AFEN values, we can find $\xi_g(x, y)$ which has the relation

$$\xi_g(x, y) = R^{-1} \phi_g(x, y). \quad (30)$$

and

$$\begin{aligned}\xi_g(x, y) &= C_g + A_{g1} SNx_g x \\ &+ A_{g2} CSx_g x A_{g3} SNx_g y + A_{g4} CSx_g y \\ &+ B_{g1} SN\frac{\sqrt{2}}{2} x_g x SN\frac{\sqrt{2}}{2} x_g y \\ &+ B_{g2} SN\frac{\sqrt{2}}{2} x_g x CS\frac{\sqrt{2}}{2} x_g y \\ &+ B_{g3} CS\frac{\sqrt{2}}{2} x_g x SN\frac{\sqrt{2}}{2} x_g y \\ &+ B_{g4} CS\frac{\sqrt{2}}{2} x_g x CS\frac{\sqrt{2}}{2} x_g y \end{aligned} \quad (31)$$

Here the above notation is given in reference 1. The coefficients of $\xi_g(x, y)$ are expressed in terms of the node-average flux, the node interface fluxes, and the corner-point fluxes.

Usually the form function method is used to reconstruct pinwise flux with $\xi_g(x, y)$. In this study, we want to solve fine-mesh difference equations with no-

dal surface flux or current. We can evaluate node surface flux or current from $\xi_g(x, y)$, which are used as boundary conditions in reconstruction. For example, the left boundary flux and current can be expressed as

$$\phi_{sg} = \phi_g(-h/2, y) = R\,\xi_g(-h/2, y), \quad (32)$$

$$J_{sg} = -D\frac{\partial}{\partial y}\phi_g(-h/2, y) = -D\,R\frac{\partial}{\partial y}\xi_g(-h/2, y). \quad (33)$$

But the surface flux and current provided by AFEN (and any other nodal codes for that matter) values are approximate. Thus the boundary conditions also contain some errors.

## 4. Numerical Tests and Results

We tested the above four boundary conditions on the EPRI-9R benchmark problem [9], which consists of heterogeneous assemblies with different types of $15\times15$ homogenized pin cells. It is a fairly realistic representation of the peripheral regions of pressurized water reactors (PWRs). This problem is rodded by a control rod cluster at the core center assembly. Therefore, there exist somewhat large flux gradients near the rodded assembly.

We verified numerically that the reconstructed flux is the same with the reference solution if the boundary conditions used are exact. In addition, when the homogeneous mixed boundary condition is used, the resulting multiplication factor is the same with the reference value.

The reference solution is from VENTURE [10] using mesh size of 0.7*cm*. We compare the four boundary conditions in terms of computing time and spectral radius of the Jacobi matrix. The iteration scheme used in this paper is LSOR and outer iteration is performed per every five inner iterations. The convergence criterion imposed is $10^{-7}$. Table 1 shows the results of the four boundary conditions. We checked that the reconstructed flux exactly matches the original reference flux.

**Table 1. Comparison of Computing Times and Spectral Radii in Rodded Assembly (Exact Boundary Conditions)**

| mesh size | boundary condition | spectral radius | computing time* (sec) |
|---|---|---|---|
| 1.4 cm | Dirichlet | 0.978411 | 0.32 |
| | Neumann | 1.001284 | 97.08 |
| | mixed(inhomogeneous) | 0.979944 | 0.36 |
| | mixed(homogeneous) | 0.980356 | 0.72 |
| 0.7cm | Dirichlet | 0.993532 | 2.34 |
| | mixed(inhomogeneous) | 0.995217 | 2.78 |
| | Neumann | 1.000296 | 350** |
| | mixed(homogeneous) | 0.995427 | 6.21 |

* Pentium-90

** HP-735 is used due to insufficient memory of Pentium-90.

The second test is reconstruction of EPRI-9R pinwise flux from AFEN values. Fig. 1 shows the groupwise maximum and average errors of pincell fluxes for the three boundary condition cases and Table 2 shows the comparison of computing times for two mesh sizes (1.4 *cm* and 0.7*cm*). We also compare the errors with that of the AFEN form function method. Fig. 2 shows groupwise surface flux and current distributions along line AB (indicated in Fig. 1), which are calculated from the AFEN values. The surface flux distribution matches well, but there are some errors at the boundary interfaced with reflector. In the

**Table 2. Comparison of Computing Times in Rodded Assembly (Reconstruction from AFEN Results)**

| mesh size | boundary condition | computing time* (sec) |
|---|---|---|
| 1.4 cm | Dirichlet | 0.40 |
| | mixed(inhomogeneous) | 0.46 |
| | mixed(homogeneous) | 1.68 |
| 0.7 cm | Dirichlet | 2.49 |
| | mixed(inhomogeneous) | 2.78 |
| | mixed(homogeneous) | 6.58 |

* Pentium-90

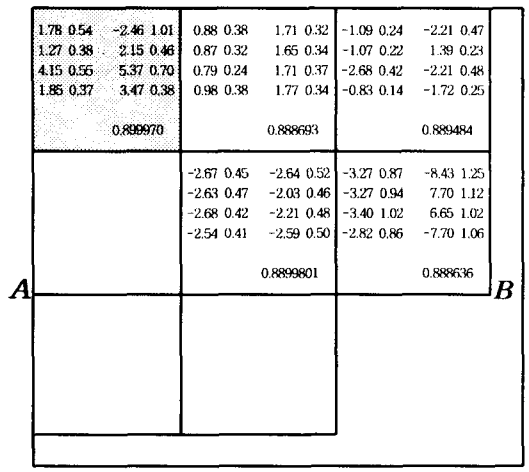


**fast** **thermal**
**maximum error(%)** **average error(%)** **maximum error(%)** **average error(%)**

| | | | | |
|---|---|---|---|---|
| x.xx | x.xx | x.xx | x.xx | AFEN form function |
| x.xx | x.xx | x.xx | x.xx | Dirichlet |
| x.xx | x.xx | x.xx | x.xx | Mixed (inhomogeneous) |
| x.xx | x.xx | x.xx | x.xx | Mixed (homogeneous) |

**eigenvalue**
x.xxxxxx Mixed (homogeneous)

◉ Reference : VENTURE (h=0.7 *cm*) $k_{eff}$ = 0.8897334
AFEN (h=21 *cm*) $k_{eff}$ = 0.8887210
◉ mesh size (h) set to 0.7 *cm*
◉ Shaded area denotes a rodded assembly
◉ Relative error : $\left( \frac{\phi_{\text{reconstructed}} - \phi_{\text{venture}}}{\phi_{\text{venture}}} \right) \times 100\ (\%)$

**Fig. 1. Maximum and Average Relative Errors of Reconstructed Pinwise Flux in EPRI-9R Benchmark Problem**

case of current, we find significant error distribution compared with that of the VENTURE reference values (that is more so in other nodal methods).

We find that the Dirichlet boundary condition and the inhomogeneous mixed boundary condition are faster than the homogeneous mixed boundary condition but that the three boundary conditions give the results of similar accuracy.

## 5. Conclusions

There are several types of boundary conditions that can be used when we reconstruct pinwise flux distribution of an assembly. We tested four boundary conditions, such as Dirichlet boundary condition, Neumann boundary condition, inhomogeneous and homogeneous mixed boundary conditions on the

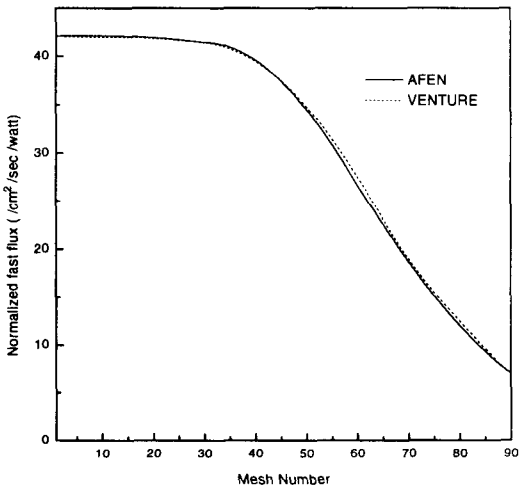


**Fig. 2a. AFEN and VENTURE Fast Flux Distribution Along Line AB**

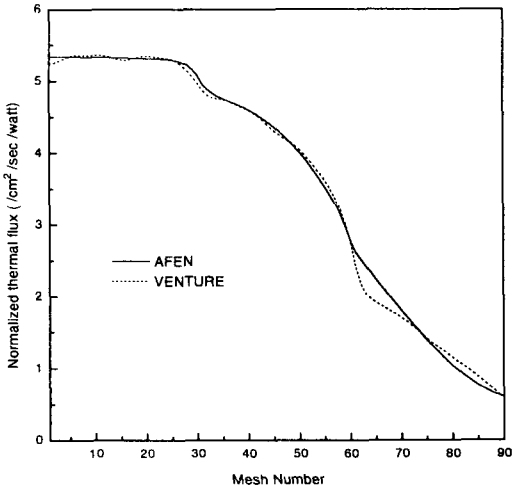


**Fig. 2b. AFEN and VENTURE Thermal Flux Distribution Along Line AB**

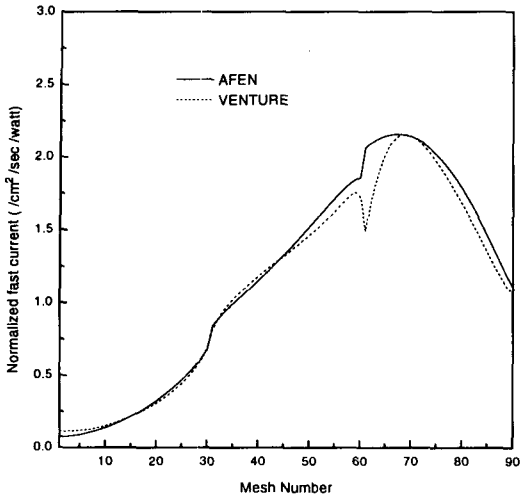


**Fig. 2c. AFEN and VENTURE Fast Current Distribution Along Line AB**

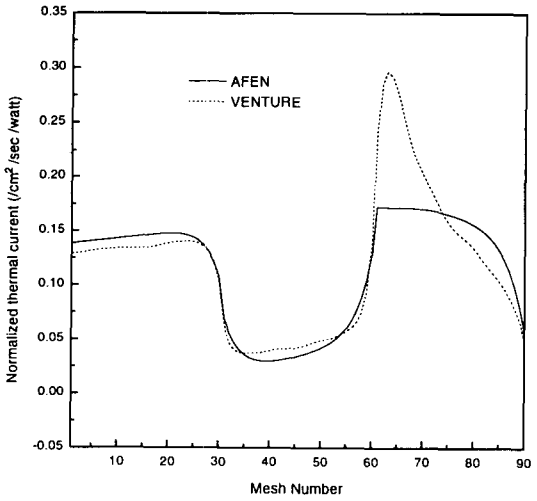


**Fig. 2d. AFEN and VENTURE Thermal Current Distribution Along Line AB**

EPRI-9R benchmark problem. The Neumann boundary condition is very prone to the ill-conditioning problem and the usual iterative methods are not applicable because the spectral radius becomes sometimes larger than one. The other boundary conditions are useful and perform reasonably well.

We have verified that the reconstructed flux exactly matches the reference solution, if the boundary conditions are exact regardless of the types.

From the results of reconstruction of the EPRI-9R benchmark problem using AFEN nodal values, we found that the Dirichlet boundary condition and the inhomogeneous mixed boundary condition are faster than the homogeneous mixed boundary condition, but with the three boundary conditions giving similar accuracy. Of the two boundary conditions (Dirichlet, inhomogeneous mixed), however, the Dirichlet boundary condition appears to be more efficient.

## References

1. J.M. Noh and N.Z. Cho, "A New Approach of Analytic Basis Function Expansion to Neutron Diffusion Nodal Calculation," *Nucl. Sci. Eng.*, **116,** 165 (1994)
2. N.Z. Cho and J.M. Noh, "Analytic Function Expansion Nodal Method for Hexagonal Geometry," *Nucl. Sci. Eng.*, **121,** 245 (1995)
3. K. Koebke and L. Hetzelt, "On the Reconstruction of Local Homogeneous Neutron Flux and Current Distributions of Light Water Reactors from Nodal Scheme," *Nucl. Sci. Eng.*, **91,** 123 (1985)
4. K.S. Smith, Spatial Homogenization Methods for Light Water Reactors, Ph.D. Thesis, Department of Nuclear Engineering, Massachusetts Institute of Technology, Cambridge, Ma. (1980)
5. K. Koebke and M.R. Wagner, "The Determination of the Pin Power Distribution in a Reactor Core on the Basis of Nodal Coarse Mesh Calculations," *Atomkernenergie.*, **30,** 136 (1977)
6. W.S. Jung and N.Z. Cho, "The Maximum Entropy Method for Reconstruction of Pointwise Neutron Flux Distribution in Nodal Methods," *Nucl. Sci. Eng.*, **108,** 384 (1991)
7. S. Nakamura, Computational Methods in Engineering and Science, John Wiley & Sons, Toronto (1977)

8. H.R. Kim and N.Z. Cho, "Global/Local Iterative Methods for Equivalent Diffusion Theory Parameters in Nodal Calculation," *Ann. Nucl. Energy*, **20**, 767 (1993)
9. C.L. Hoxie, Applications of Nodal Equivalence Theory to the Neutronic Analysis of PWR's, Ph. D. Thesis, Massachusetts Institute of Technology, Cambridge, Ma. (1982)
10. D.R. Vondy et.al., "VENTURE : A Code Block for Solving Multigroup Neutronic Problems Applying the Finite-Difference Diffusion-Theory Approximation to Neutron Transport-Version Ⅱ," ORNL-5062/R1, Oak Ridge National Laboratory (1977)